QCD Splitting/Joining Functions at Finite Temperature in the Deep LPM Regime

Peter Arnold and Çağlar Doğan

Department of Physics, University of Virginia, Box 400714, Charlottesville, Virginia 22904, USA (Dated: April 15, 2019)

Abstract

There exist full leading-order-in- α_s numerical calculations of the rates for massless quarks and gluons to split and join in the background of a quark-gluon plasma through hard, nearly collinear bremsstrahlung and inverse bremsstrahlung. In the limit of partons with very high energy E, where the physics is dominated by the Landau-Pomeranchuk-Migdal (LPM) effect, there are also analytic leading-log calculations of these rates, where the logarithm is $\ln(E/T)$. We extend those analytic calculations to next-to-leading-log order. We find agreement with the full result to within roughly 20% for $E_{<} \gtrsim 10T$, where $E_{<}$ is the energy of the least energetic parton in the splitting/joining process. We also discuss how to account for the running of the coupling constant in the case that E/T is very large. Our results are also applicable to isotropic non-equilibrium plasmas if the plasma does not change significantly over the formation time associated with particle splitting.

I. INTRODUCTION AND RESULTS

When very high energy particles travel through a quark-gluon or electromagnetic plasma, the dominant energy loss mechanism is through hard bremsstrahlung or pair creation, similar to the cascading of high energy cosmic rays in the atmosphere or of a high energy particle in a calorimeter. It was long a problem of interest to calculate the rate for such splitting processes in the formal limit of very high temperature quark-gluon plasmas, where the running strong coupling $\alpha_s(T)$ can be treated as small [1, 2, 3, 4, 5, 6]. The problem is complicated by the Landau-Pomeranchuk-Migdal (LPM) effect [7] (reviewed below): for very high energy particles, the quantum mechanical duration of the splitting process exceeds the mean free time between collisions, and so successive collisions cannot be treated independently.

For the case of approximately on-shell massless particles traveling through an infinite medium, a complete leading-order analysis of such processes was carried out by Jeon and Moore [6] using the formalism of Arnold, Moore, and Yaffe (AMY) [8, 9, 10]. This analysis requires substantial numerical work to solve integral equations describing the LPM effect. Where possible, it's always nice to have analytic results in place of numerical results, because they are simpler to calculate and because they can facilitate comparison between different approaches. One case where analytic results can be found, explored in earlier literature, is the limit where the particle momentum p is so large compared to the plasma temperature Tthat the inverse logarithm $1/\ln(p/T)$ can be treated as a small number. We will refer to this as the deep LPM regime. In the limit of small α_s , earlier authors have given analytic results for splitting processes to leading order in powers of this inverse logarithm.¹ (In contrast, the work of Jeon and Moore made no assumption about the size of the logarithm, and holds both in and out of the deep LPM limit, to leading order in coupling α_s .) The difficulty with leading-log results is that for practical purposes there is a huge difference, for example, between $\ln(p/T)$ and $\ln(p/4\pi^2T)$ if p is of order 10–100 T. But a leading-log analysis will not distinguish between these two situations since $\ln(p/4\pi^2T) = \ln(p/T) + O(1)$. Consider, for example, 5-20 GeV jets at early times in a RHIC collision, with temperatures of order 300 MeV. As a general rule, one almost always needs to push expansions in inverse logarithms to next-to-leading-log order to get useful results.

Our goal is to find analytic results for splitting processes to next-to-leading logarithmic (NLL) order in the deep LPM regime. In this paper, we make a first step towards that goal by computing the next-to-leading logarithmic result in the formal parametric limit that $T \ll p \ll T/[\alpha_{\rm s}^2 \ln(\alpha_{\rm s}^{-1})]$ for weak coupling: that is, deep in the LPM regime, but not too deep. We will leave the more involved calculation of NLL results for higher energy particles $p \gtrsim T/[\alpha_{\rm s}^2 \ln(\alpha_{\rm s}^{-1})]$ for future work. However, later in this paper (section VIA), we will see that NLL results for higher-energy particles will differ by only about 15% from the formulas derived here. In this paper we will also discuss leading-log results in the case of extremely high energy particles, where P is so large that there is significant difference between the running couplings $\alpha_{\rm s}(P)$ and $\alpha_{\rm s}(T)$.

As we will discuss later, our results apply not just to equilibrium plasmas but more generally to plasmas with an isotropic distribution of particle momenta (in which case the "T" in our discussion refers to the typical energy scale of plasma particles). We express our answers in terms of the splitting functions $\gamma_{a\leftrightarrow bc}(P;xP,(1-x)P)$ of Refs. [9, 10],² which

¹ See Eqs. (19–20) of Ref. [11], which is based on the earlier work of Refs. [1, 4, 5].

We use the term "splitting functions" to describe the functions γ in the splitting rate (1.1). Though

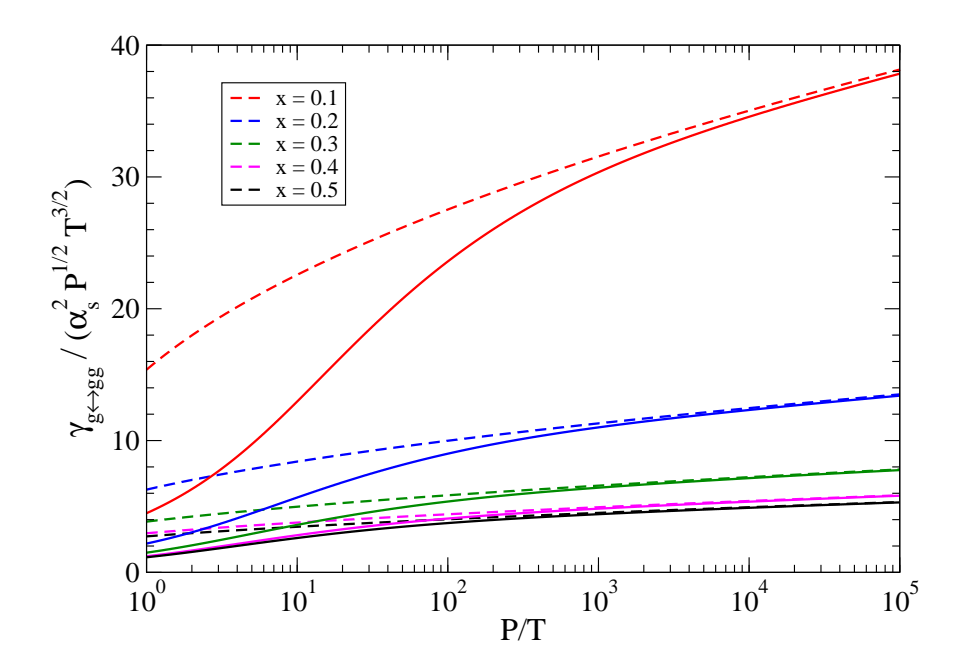


FIG. 1: Exact (solid line) and next-to-leading logarithmic order (dashed line) results for $\gamma_{g\leftrightarrow gg}$ at leading order in coupling α_s for QCD with three massless flavors ($N_f=3$). $\gamma_{g\leftrightarrow gg}$ is plotted in units of $\alpha_s^2 P^{1/2} T^{3/2}$ as a function of P/T for various values of x, where P is the momentum of the initial high-energy particle and xP and (1-x)P are the momenta after splitting. From top to bottom, the curves corresponds to x=0.1, 0.2, 0.3, 0.4, 0.5.

are defined so that the rate per particle of type i and momentum P for that particle to split into particles of type j and k and momentum fractions x and 1-x is³

$$\frac{d\Gamma_{a\to bc}}{dx} = \frac{(2\pi)^3}{2P\nu_a} \gamma_{a\leftrightarrow bc} (P; xP, (1-x)P) [1 \pm f_b(xP)] [1 \pm f_c((1-x)P)]. \tag{1.1}$$

Here f(p) is the phase space distribution of plasma particles of a given type, and the factors $1 \pm f(p)$ are Bose enhancement or Fermi blocking factors. In equilibrium, $f(p) = 1/(e^{\beta p} \mp 1)$ is the Bose or Fermi distribution associated with (massless) particles of a given type. ν_a is the number of spin times color states for particle type a (i.e. 6 for a quark or anti-quark and 16 for a gluon). The prefactors in (1.1) are just convenient normalization conventions in the definition of $\gamma_{a \leftrightarrow bc}$.

We will give the formula for our next-to-leading-log (NLL) result in Sec. III, after a qualitative review of the form of the leading-log result. For now, we offer in Fig. 1 a numerical comparison of the NLL computation to the full leading-order-in- $\alpha_{\rm s}$ formula of Refs. [9, 10] for the case of gluon splitting $g \leftrightarrow gg$. Formally, both of these curves assume weak coupling and that P is parametrically small compared to $T/[\alpha_{\rm s}^2 \ln(\alpha_{\rm s}^{-1})]$. Obviously, for any phenomenologically interesting values of $\alpha_{\rm s}$, the last assumption is rather unlikely to be valid for the momenta $P \sim 10^5 \, T$ shown at the far right of the plot. We extend the plot

there is some connection, they should not be confused with the DGLAP splitting functions familiar from zero-temperature QCD. Also, in the notation of Refs. [9, 10], this would be $\gamma_{bc}^a(P; xP, (1-x)P)$.

³ Readers of Ref. [6] should note that we use the symbol Γ to denote rate per particle, whereas Ref. [6] denotes this by $d\Gamma/dt$.

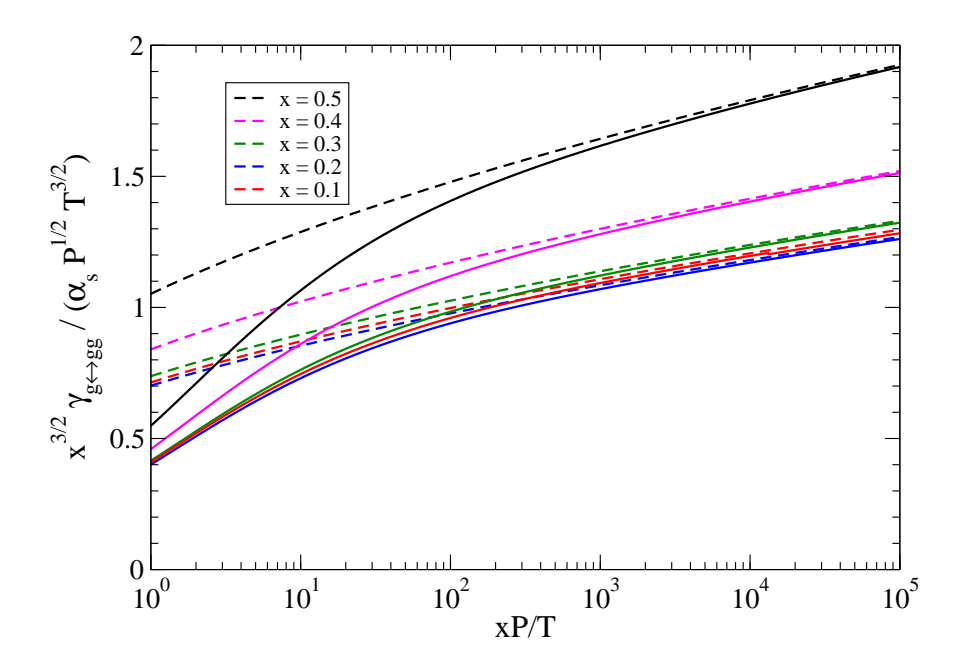


FIG. 2: As Fig. 1 but the horizontal axis shows $p_{<}/T$, which is xP/T for the x values used to label the curves, and the vertical axis has been rescaled by a factor of $x^{3/2}$. From top to bottom, the curves corresponds to x = 0.5, 0.4, 0.3, 0.1, 0.2.

this far simply to show that the NLL curve is successfully approaching the more complete numerical calculation based on the same assumption, as it must.

To summarize how well the NLL expansion works, it is useful to rescale the plot as in Fig. 2. Here, the horizontal axis shows the smallest of the two final momenta,

$$p_{<} \equiv \min(xP, (1-x)P), \tag{1.2}$$

instead of the initial particle momentum P, and the vertical axis has been scaled with x in a way that shows the limiting small x behavior by collapsing small x curves atop each other. For $p_{<} \simeq 100T$, the NLL result differs from the full leading-order formula by roughly 5%. For $p_{<} \simeq 10T$, the difference is roughly 20%. Pushing the expansion in inverse logarithms down to $p_{<}/T \simeq 1$, where one would not expect it to be useful, we see that the NLL result gives the right order of magnitude but is off by a factor of roughly 2. We conclude that the NLL approximation for gluon splitting in an infinite medium is reasonable for $p_{<} \gtrsim 10T$.

In the next section, we will set up our discussion by giving a brief qualitative review of the basic parametric scales associated with the LPM effect in a quark-gluon plasma. We also discuss the reason for the parametric assumption $P \ll T/[\alpha_{\rm s}^2 \ln(\alpha_{\rm s}^{-1})]$ in our analysis: In this limit, it turns out that the momentum transfer due to scattering during a splitting process is small compared to the O(T) momenta of typical plasma particles, which greatly simplifies the analysis. In section III, we present the formulas for our NLL result, followed by their derivation in section IV. In section V, we compare numerical results for processes besides the $g \to gg$ splitting presented above.

We should clarify that throughout most of this paper, we work to leading order in powers of the coupling α_s . In particular, the phrase "leading logarithm" will mean the leading logarithmic contribution at leading order in α_s . It does not mean a sum of leading logarithms at all orders in α_s . The phrase next-to-leading logarithm will be used similarly, and does not include any resummation of effects higher order in α_s .

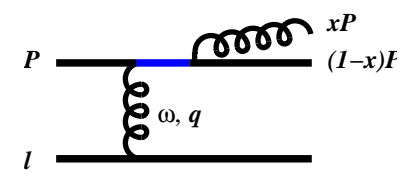


FIG. 3: A diagram contributing to bremsstrahlung from a single collision.

In particular, our NLL results will formally assume that $\ln(P/T)$ is parametrically large but that $\alpha_{\rm s} \ln(P/T)$ is parametrically small. In section VI, we discuss what to do when $\alpha_{\rm s} \ln(P/T)$ is not small. This is equivalent to a discussion of what renormalization scale should be used when evaluating $\alpha_{\rm s}$. In this section, we necessarily abandon the $P \ll T/[\alpha_{\rm s}^2 \ln(\alpha_{\rm s}^{-1})]$ restriction, considering much higher momentum scales, but we will only work to leading log order.

II. QUALITATIVE REVIEW OF LEADING-LOG RESULT

A. Basic Parametric Estimates

Before presenting our next-to-leading-log results, it is useful to first qualitatively review the form of leading-log results. For definiteness, we'll consider the case of gluon bremsstrahlung. Splitting can occur when nearly collinear bremsstrahlung accompanies a small-angle scattering of the high energy particle off of a plasma particle, such as depicted by the diagram of Fig. 3 for a momentum P particle splitting into two particles of momentum $k \simeq xP$ and $p \simeq (1-x)P$. The intermediate solid line in this diagram is off-shell in energy by an amount of order

$$\delta E \equiv E_{p} + E_{k} - E_{p+k}
\simeq \frac{p_{\perp}^{2} + m^{2}}{2p} + \frac{k_{\perp}^{2} + m_{g}^{2}}{2k} - \frac{|\mathbf{p}_{\perp} + \mathbf{k}_{\perp}|^{2} + m^{2}}{2(p+k)}
\simeq \frac{p_{\perp}^{2} + m^{2}}{2xP} + \frac{k_{\perp}^{2} + m_{g}^{2}}{2(1-x)P} - \frac{|\mathbf{p}_{\perp} + \mathbf{k}_{\perp}|^{2} + m^{2}}{2P} .$$
(2.1)

For simplicity, in this review section we'll focus on the case $x \sim 0.5$ (that is, neither x nor 1-x very small). In a typical bremsstrahlung process, the relative angle between \boldsymbol{p} and \boldsymbol{k} is the same order of magnitude as the angle of deflection in the initiating small-angle scattering process.⁴ For $x \sim 0.5$, then

$$\delta E \sim \frac{Q_{\perp}^2 + (\text{masses})^2}{P},$$
 (2.2)

where Q_{\perp} is the size of the momentum transfer (transverse to the high energy particle's direction of motion) in the underlying scattering process. Thermal particle masses are of

⁴ For larger angles between p and k, there is a cancellation between the amplitudes for initial and final state radiation. In vacuum, bremsstrahlung can be logarithmically dominated by smaller angles between p and k, giving rise to a collinear logarithmic enhancement of the bremsstrahlung rate. This is nor relevant to the deep LPM limit, however, for reasons that will be reviewed in footnote 7.

order gT, and the relevant range of Q_{\perp} is bounded below by the Debye screening mass of order gT. So we can simplify the parametric estimate (2.2) to

$$\delta E \sim \frac{Q_{\perp}^2}{P} \,. \tag{2.3}$$

The quantum duration $1/\delta E$ of the Bremsstrahlung process is called the "formation" time of the Bremsstrahlung gluon:

$$t_{\text{form}} \sim \frac{1}{\delta E} \sim \frac{P}{Q_{\perp}^2} \,.$$
 (2.4)

In the limit of large P, this time will become larger than the mean free time between collisions, and successive collisions can no longer be treated as quantum mechanically independent for the calculation of bremsstrahlung. As far as bremsstrahlung is concerned, the multiple collisions during the formation time have roughly the same effect as a single collision with the same total momentum transfer Q_{\perp} as the multiple collisions. So, on the one hand, the formation time is given by (2.4). On the other hand, it is also the time t_{coll} for multiple collisions to generate a total momentum transfer of size Q_{\perp} , which is given by

$$t_{\rm coll}^{-1} \sim n \,\sigma_1(Q_\perp) \,\ln\left(\frac{Q_\perp}{m_{\rm D}}\right) \sim \frac{g^4 T^3}{Q_\perp^2} \,\ln\left(\frac{Q_\perp}{m_{\rm D}}\right).$$
 (2.5)

Here, $n \sim T^3$ is the density of particles to scatter from, and $\sigma_1(Q_\perp) \sim g^4/Q_\perp^2$ is the cross-section for a *single* Coulomb-like scattering with momentum transfer of order Q_\perp . The logarithmic enhancement to the rate $t_{\rm coll}^{-1}$ is known as a Coulomb logarithm, which accounts for the fact that a given total momentum transfer can occur not only through a single collision, but also through multiple collisions which each individually transfer less momentum but occur more frequently.⁶ Self-consistently equating (2.4) and (2.5),

$$\frac{P}{Q_{\perp}^2} \sim t_{\text{form}} \sim t_{\text{coll}} \sim \frac{Q_{\perp}^2}{g^4 T^3 \ln(Q_{\perp}/m_{\text{D}})}.$$
 (2.6)

This determines the total Q_{\perp} and thence t_{form} and t_{coll} . Finally, we want the rate for bremsstrahlung. Every time increment t_{coll} , we produce effectively one net collision from the point of view of a potential bremsstrahlung gluon. The cost of adding a gluon emission to a scattering process is parametrically a factor⁷ of g^2 . So the rate for bremsstrahlung is of order g^2/t_{coll} , except that we need to include final state factors $1 \pm f$:

$$\Gamma_{\text{brem}} \sim \frac{g^2}{t_{\text{coll}}} \times \text{(final state factors)}.$$
 (2.7)

For a review of these scales in extremely simple language, see Sec. 4.5.1 of Ref. [12] in the context of $P \sim T$. For a more serious discussion in the deep LPM regime, see for example Sec. 4.1 of Ref. [2], where the translation to the present discussion is that their mean free path λ for $2\rightarrow 2$ scattering is of order $1/(g^2T)$ and their inverse screening length μ is of order gT.

⁶ For a textbook discussion of Coulomb logarithms, see Ref. [13].

⁷ For bremsstrahlung from a single collision in vacuum, there is also generally both an infrared logarithmic enhancement, associated with integrating over small x, and a collinear logarithmic enhancement, previously mentioned in footnote 4. The infrared behavior need not be considered here because we are restricting attention to $x \sim 0.5$ in this qualitative discussion. (Note also that the discussion of the infrared in medium would be different from the vacuum case because of the final state factor 1 + f for the bremsstrahlung particle.) The collinear logarithm in the vacuum case depends on the initial and final

Our qualitative discussion in this section has been for $x \sim 0.5$, and the Γ_{brem} above is implicitly integrated over x's of this order. Comparing to (1.1), the splitting functions that we defined earlier are then of order

$$\gamma \sim \frac{g^2 P}{t_{\text{coll}}} \sim g^2 Q_\perp^2. \tag{2.8}$$

We can now determine Q_{\perp} self-consistently from (2.6) and thence the splitting function via (2.8).

B. Preview of the inverse log expansion

To make the leading-log expansion more explicit, it's helpful to note that the Debye mass m_D is of order gT and rewrite the parametric equation (2.6) for Q_{\perp} in the form

$$\hat{Q}_{\perp}^2 \sim \left(\frac{P}{T}\right)^{1/2} \ln^{1/2}(\hat{Q}_{\perp}^2),$$
 (2.9)

where

$$\hat{Q}_{\perp} \equiv \frac{Q_{\perp}}{m_{\rm D}} \,, \tag{2.10}$$

and then expand the solution for \hat{Q}_{\perp} by iteration. First ignore the logarithm and define $\hat{Q}_{\perp 0}$ by the corresponding solution

$$\hat{Q}_{\perp 0}^2 \sim \left(\frac{P}{T}\right)^{1/2}.$$
 (2.11)

Plugging this into the right-hand side of (2.9) gives an improved solution

$$\hat{Q}_{\perp}^2 \sim \left(\frac{P}{T}\right)^{1/2} \ln^{1/2}(\hat{Q}_{\perp 0}^2)$$
 (2.12)

So

$$\hat{Q}_{\perp}^2 \sim \left(\frac{P}{T}\right)^{1/2} \ln^{1/2} \left(\frac{P}{T}\right), \tag{2.13}$$

and the splitting function (2.8) is

$$\gamma \sim g^2 m_{\rm D}^2 \hat{Q}_{\perp}^2 \sim g^4 T^2 \left(\frac{P}{T}\right)^{1/2} \ln^{1/2} \left(\frac{P}{T}\right).$$
 (2.14)

The inverse logarithm expansion is predicated on the assumption that the logarithm in (2.12) and (2.13) is large. As an example, supposed we plug the approximation (2.12) back

state particles traveling in straight lines for sufficiently long distances before and after the collision. It does not arise in the LPM regime because $t_{\rm coll} \sim t_{\rm form}$. In any case, we will shortly turn to specific results rather than rough parametric estimates, and the only logarithm that one finds in the answer is the Coulomb logarithm in (2.5).

into the right-hand side of (2.9) to get a new approximation for \hat{Q}_{\perp} :

$$\hat{Q}_{\perp}^{2} \sim \left(\frac{P}{T}\right)^{1/2} \ln^{1/2} \left[\left(\frac{P}{T}\right)^{1/2} \ln^{1/2} (\hat{Q}_{\perp 0}^{2}) \right]$$

$$= \left(\frac{P}{T}\right)^{1/2} \left[\ln \left(\frac{P}{T}\right) + \ln \ln(\hat{Q}_{\perp 0}^{2}) \right]^{1/2}. \tag{2.15}$$

In the limit that $\ln(P/T) \gg 1$, then $\ln(P/T)$ is also large compared to $\ln \ln(\hat{Q}_{\perp 0}^2) \sim \ln \ln(P/T)$. So we may formally choose to think of the double-log correction as part of the next-to-leading order terms in the expansion in inverse logs.

C. The parametric assumption $P \ll T/[\alpha_s^2 \ln(\alpha_s^{-1})]$

As we'll discussion in section IVA, the NLL calculation will be much simpler if the momentum transfers in individual scattering events can be treated as a small perturbation to typical particles in the plasmas. The relevant transverse momentum transfers q_{\perp} of individual collisions range from order $m_{\rm D}$ to order Q_{\perp} , which gives rise to the Coulomb logarithm in (2.5). So the simplifying assumption that $q_{\perp} \ll T$ is equivalent to $Q_{\perp} \ll T$ in our analysis. From (2.9), this is

$$\frac{T^2}{m_{\rm D}^2} \gg \left(\frac{P}{T}\right)^{1/2} \ln^{1/2} \left(\frac{T^2}{m_{\rm D}^2}\right),$$
(2.16)

which in turn is

$$P \ll \frac{T^5}{m_{\rm D}^4 \ln(T^2/m_{\rm D}^2)} \sim \frac{T}{g^4 \ln(1/g)}.$$
 (2.17)

In weak coupling, the simplifying assumption that momentum transfers are small compared to T is therefore parametrically $P \ll T/[\alpha_s^2 \ln(\alpha_s^{-1})]$.

III. OUR NLL RESULT

Our next-to-leading-logarithm result can be summarized in the following form:

$$\gamma_{g \leftrightarrow gg}(P; xP, (1-x)P) = \frac{d_{\mathcal{A}}C_{\mathcal{A}}\alpha_{s}}{(2\pi)^{4}\sqrt{2}} m_{\mathcal{D}}^{2} \hat{\mu}_{\perp}^{2}(1, x, 1-x; \mathcal{A}, \mathcal{A}, \mathcal{A}) \frac{1+x^{4}+(1-x)^{4}}{x^{2}(1-x)^{2}}, \quad (3.1a)$$

$$\gamma_{q \leftrightarrow gq}(P; xP, (1-x)P) = \frac{d_{\rm F}C_{\rm F}\alpha_{\rm s}}{(2\pi)^4\sqrt{2}} m_{\rm D}^2 \hat{\mu}_{\perp}^2(1, x, 1-x; F, A, F) \frac{1+(1-x)^2}{x^2(1-x)},$$
(3.1b)

$$\gamma_{g \leftrightarrow q\bar{q}}(P; xP, (1-x)P) = \frac{d_{\rm F}C_{\rm F}\alpha_{\rm s}}{(2\pi)^4\sqrt{2}} m_{\rm D}^2 \hat{\mu}_{\perp}^2(1, x, 1-x; A, F, F) \frac{x^2 + (1-x)^2}{x(1-x)}$$
(3.1c)

(per quark flavor),

where $\hat{\mu}^2$ $(x_1, x_2, x_3; s_1, s_2, s_3)$ solves the equation

$$\hat{\mu}_{\perp}^{2} = \frac{gT}{m_{D}} \left[\frac{2}{\pi} x_{1} x_{2} x_{3} \frac{P}{T} \right]^{1/2} \left[\frac{1}{2} (C_{s_{2}} + C_{s_{3}} - C_{s_{1}}) x_{1}^{2} \ln \left(\frac{\xi \hat{\mu}_{\perp}^{2}}{x_{1}^{2}} \right) + \frac{1}{2} (C_{s_{3}} + C_{s_{1}} - C_{s_{2}}) x_{2}^{2} \ln \left(\frac{\xi \hat{\mu}_{\perp}^{2}}{x_{2}^{2}} \right) + \frac{1}{2} (C_{s_{2}} + C_{s_{3}} - C_{s_{1}}) x_{3}^{2} \ln \left(\frac{\xi \hat{\mu}_{\perp}^{2}}{x_{3}^{2}} \right) \right]^{1/2},$$
(3.2)

 ξ is the constant

$$\xi \equiv \exp\left(2 - \gamma_{\rm E} + \frac{\pi}{4}\right) \simeq 9.09916\,,\tag{3.3}$$

 $\gamma_{\rm E}$ is the Euler-Mascheroni constant, and the other constants will be defined in a moment. Schematically, these equations are of the form (2.9) and (2.14) with $\hat{\mu}_{\perp}$ playing the role of \hat{Q}_{\perp} . The appearance of three different logarithms can be roughly understood as arising because there are three different particle momenta in the problem: P, xP, and (1-x)P. (In contrast, the earlier qualitative discussion was only about orders of magnitude and took $x \sim 0.5$.) The various explicit functions of x at the ends of Eqs. (3.1) are simply the usual vacuum DGLAP splitting functions divided by x(1-x). The role of the medium, both in terms of providing the momentum transfer and the LPM effect, is contained in $m_{\rm D}^2\hat{\mu}_{\perp}^2$.

The reason we have switched notation from \hat{Q}_{\perp} to $\hat{\mu}_{\perp}$ is because there are several different transverse momenta in the problem, associated with the three different particles, and each of them has a distribution of values rather than a single well-defined value. We did not want to give the impression that $\hat{\mu}_{\perp}$ exactly corresponded to a particular transverse momentum in the problem. For $x \sim 0.5$, $\hat{\mu}_{\perp}$ is the same order of magnitude as the \hat{Q}_{\perp} scale we identified in earlier discussion, but one could just as well redefine the normalization of $\hat{\mu}_{\perp}$ by replacing the symbol $\hat{\mu}_{\perp}$ by $c\hat{\mu}_{\perp}$ everywhere on both sides of equations (3.1) and (3.2), for some numerical constant c.

In the preceding equations, $C_{\rm F}$ and $C_{\rm A}$ are the quadratic Casimirs, and $d_{\rm F}$ and $d_{\rm A}$ are the dimensions, of the fundamental and adjoint color representations. It's also convenient to define the trace normalization factor t_R by ${\rm tr}(T_R^aT_R^b)=t_R\delta^{ab}$, where T_R^a are color generators. In general, $t_R=d_RC_R/d_A$ and $t_{\rm A}=C_{\rm A}$. For QCD,

$$C_{\rm F} = \frac{4}{3}$$
, $C_{\rm A} = 3$, $d_{\rm F} = 3$, $d_{\rm A} = 8$, $t_{\rm F} = \frac{1}{2}$, $t_{\rm A} = 3$. (3.4)

For QCD with $N_{\rm f}$ massless fermion flavors, the Debye mass is given by

$$m_{\rm D}^2 = \left(t_{\rm A} + N_{\rm f} t_{\rm F}\right) \frac{1}{3} g^2 T^2 = \left(1 + \frac{1}{6} N_{\rm f}\right) g^2 T^2.$$
 (3.5)

Also, the $\gamma_{g\leftrightarrow q\bar{q}}$ formula in (3.1c) is for a single flavor of quark in the final state, and so (1.1) should be multiplied by a factor of $N_{\rm f}$ if one wants the total rate for a gluon to split into any $q\bar{q}$ pair.

One can formally expand in powers of inverse logarithms by solving (3.2) by iteration, as discussed qualitatively in section Sec. II B. If some initial guess $\hat{Q}_{\perp 0} \sim (P/T)^{1/2}$ is made for $\hat{\mu}_{\perp}$, then the iterated approximations are

$$\hat{\mu}_{\perp 1}^2 = R(\hat{Q}_{\perp 0}^2),\tag{3.6}$$

$$\hat{\mu}_{\perp 2}^2 = R(\hat{\mu}_{\perp 1}^2) = R(R(\hat{Q}_{\perp 0}^2)), \tag{3.7}$$

where $R(\hat{\mu}_{\perp}^2)$ represents the right-hand side of (3.2). The result $\hat{\mu}_{\perp 2}$ is valid to next-to-leading-log order and is actually the form we derive our result in later in this paper. If one changes the initial guess $\hat{Q}_{\perp 0}$ by an O(1) multiplicative factor, it only affects the result for $\hat{\mu}_{\perp 2}$ at yet higher order in the inverse logarithm expansion. That's fine as a theoretical statement, but it leaves ambiguous how to choose $\hat{Q}_{\perp 0}$ for numerical comparisons such as Figs. 1 and 2. We therefore re-organized our result into the natural form (3.2), which provides a specific prescription for determining $\hat{\mu}_{\perp}$. The slight cost is that, instead of a closed form expression like (3.7) for the NLL result, we have a simple implicit algebraic equation (3.2) for $\hat{\mu}_{\perp}$ that needs to be solved numerically.

IV. DETAILS OF THE CALCULATION

A. The equations to solve

We will work in the formalism of Ref. [9, 10]. In their notation, the functions $\gamma_{a\leftrightarrow bc}$ describing nearly collinear splitting/joining are

$$\gamma_{q \leftrightarrow qg}(\bar{p}'; \bar{p}, \bar{k}) = \gamma_{\bar{q} \leftrightarrow \bar{q}g}(\bar{p}'; \bar{p}, \bar{k}) = \frac{\bar{p}'^2 + \bar{p}^2}{\bar{p}'^2 \, \bar{p}^2 \, \bar{k}^3} \, \mathcal{F}_{q}(\bar{p}', \bar{p}, \bar{k}) \,, \tag{4.1a}$$

$$\gamma_{g \leftrightarrow q\bar{q}}(\bar{p}'; \bar{p}, \bar{k}) = \frac{\bar{k}^2 + \bar{p}^2}{\bar{k}^2 \, \bar{p}^2 \, \bar{p}'^3} \, \mathcal{F}_{q}(\bar{k}, -\bar{p}, \bar{p}') \,, \tag{4.1b}$$

$$\gamma_{g \leftrightarrow gg}(\bar{p}'; \bar{p}, \bar{k}) = \frac{\bar{p}'^4 + \bar{p}^4 + \bar{k}^4}{\bar{p}'^3 \bar{p}^3 \bar{k}^3} \mathcal{F}_{g}(\bar{p}', \bar{p}, \bar{k}), \qquad (4.1c)$$

where

$$\mathcal{F}_s(p', p, k) \equiv \frac{d_s C_s \alpha}{2(2\pi)^3} \int \frac{d^2 h}{(2\pi)^2} 2\mathbf{h} \cdot \text{Re} \, \mathbf{F}_s(\mathbf{h}; p', p, k). \tag{4.2}$$

Here F_s is the solution to the following integral equation

$$2\mathbf{h} = i \, \delta E(\mathbf{h}; p', p, k) \, \mathbf{F}_s(\mathbf{h}; p', p, k)$$

$$+ g^2 \int \frac{d^2 q_\perp}{(2\pi)^2} \, \mathcal{A}(q_\perp) \left\{ \frac{1}{2} C_{\mathcal{A}} \left[\mathbf{F}_s(\mathbf{h}; p', p, k) - \mathbf{F}_s(\mathbf{h} + p' \mathbf{q}_\perp; p', p, k) \right] \right.$$

$$+ \left. \left(C_s - \frac{1}{2} C_{\mathcal{A}} \right) \left[\mathbf{F}_s(\mathbf{h}; p', p, k) - \mathbf{F}_s(\mathbf{h} - k \mathbf{q}_\perp; p', p, k) \right] \right.$$

$$+ \left. \frac{1}{2} C_{\mathcal{A}} \left[\mathbf{F}_s(\mathbf{h}; p', p, k) - \mathbf{F}_s(\mathbf{h} - p \mathbf{q}_\perp; p', p, k) \right] \right\}, \tag{4.3}$$

which we will refer to as the LPM equation. In this equation,

$$\delta E(\mathbf{h}; p', p, k) = \frac{m_{\text{eff,g}}^2}{2k} + \frac{m_{\text{eff,s}}^2}{2p} - \frac{m_{\text{eff,s}}^2}{2p'} + \frac{h^2}{2pkp'}$$
(4.4)

represents the energy denominator $E_{g,k} + E_{s,p} - E_{s,p'}$ in a $p' \leftrightarrow pk$ splitting/joining process. Here, $m_{\text{eff},s}$ is the O(gT) effective thermal mass of hard particles of species s.⁸ The two-dimensional vector \boldsymbol{h} is related to transverse momentum and physically corresponds to the

⁸ We will not need explicit formulas for $m_{\text{eff},s}$ in this paper.

combination

$$\boldsymbol{h} = k\boldsymbol{p}_{\perp} - p\boldsymbol{k}_{\perp}.\tag{4.5}$$

In terms of the qualitative discussion of Sec. II, one can crudely think of the order of magnitude of h as representing $h \sim PQ_{\perp}$. The function $\mathcal{A}(q_{\perp})$ is the integrated correlator

$$\mathcal{A}(\boldsymbol{q}_{\perp}) = \int \frac{dq_z}{2\pi} \left\langle \left\langle A^{-}(\omega, \boldsymbol{q}_{\perp}, q_z) [A^{-}(\omega, \boldsymbol{q}_{\perp}, q_z)]^* \right\rangle \right\rangle \bigg|_{\omega = q_z}, \tag{4.6}$$

where $A^- \equiv A^0 - A^z$ and $\langle \langle AA^* \rangle \rangle$ is the thermal Wightman gauge field correlator (neglecting the momentum-conserving δ -function). If momentum transfers are small compared to typical plasma particle momenta, then one may evaluate the self-energies in this correlator in the hard thermal loop approximation. For the case of equilibrium, \mathcal{A} then has the simple form [14]

$$\mathcal{A}(q_{\perp}) = T\left(\frac{1}{q_{\perp}^2} - \frac{1}{q_{\perp}^2 + m_{\rm D}^2}\right) = \frac{Tm_{\rm D}^2}{q_{\perp}^2(q_{\perp}^2 + m_{\rm D}^2)}.$$
 (4.7)

As discussed in Ref. [9], the last formula holds more generally for the case of any homogeneous plasma where the distribution of plasma particle momenta is isotropic. The "temperature" and Debye mass to use in (4.7) in such a situation are⁹

$$T = T_* \equiv \frac{\sum_s \bar{\nu}_s t_s \int \frac{d^3 p}{(2\pi)^3} f_s(p) [1 \pm f_s(p)]}{2 \sum_s \bar{\nu}_s t_s \int \frac{d^3 p}{(2\pi)^3} \frac{f_s(p)}{p}},$$
(4.8)

$$m_{\rm D}^2 = 2g^2 \sum_s \bar{\nu}_s t_s \int \frac{d^3 p}{(2\pi)^3} \frac{f_s(p)}{p},$$
 (4.9)

where $\bar{\nu}_s \equiv \nu_s/d_s$ is the number of degrees of freedom of a species s excluding color; $f_s(p)$ is the phase space distribution of particle of type s per spin and color degree of freedom; and the species sum is over gluons, flavors of quarks, and flavors of anti-quarks. For our analysis of splitting processes, this generalization to isotropic non-equilibrium situations will only be valid if the plasma particle distribution functions do not significantly change over the course of a formation time.

The simple form (4.7) for $\mathcal{A}(q_{\perp})$ is justified by our parametric assumption $P \ll T/[\alpha_{\rm s}^2 \ln(\alpha_{\rm s}^{-1})]$. We will give some discussion of what happens at higher P in section VI, but we leave a full NLL calculation at higher P for future work.

In (4.3), the variable \mathbf{q}_{\perp} represents the transverse momentum exchange from individual $2\rightarrow 2$ scattering processes. Solving the integral equation for \mathbf{F}_s then accounts for summing up multiple scattering into the LPM effect. For a discussion with notation similar to that used in this paper, see, for example, Ref. [8].

B. The leading log solution

The Coulomb logarithm arises in the LPM equation (4.3) from the region of \mathbf{q}_{\perp} integration where $m_{\rm D} \ll q_{\perp}$ with q_{\perp} still small enough that $\mathbf{h} + p'\mathbf{q}_{\perp}$, $\mathbf{h} - k\mathbf{q}_{\perp}$ and/or $\mathbf{h} - p\mathbf{q}_{\perp}$ are

For QCD with $N_{\rm f}$ flavors, and identical distributions of all quarks and anti-quarks, this would be $T_* = g^2 \int \frac{d^3p}{(2\pi)^3} \left[6f_g(1+f_g) + 2N_{\rm f}f_q(1-f_q) \right]/m_{\rm D}^2$ and $m_{\rm D}^2 = 2g^2 \int \frac{d^3p}{(2\pi)^3} \left[6f_g + 2N_{\rm f}f_q \right]/p$.

still close to h. Roughly speaking, this is the approximation that the important momentum transfers q_{\perp} from individual collisions are large compared to $m_{\rm D}$ but small compared to the total Q_{\perp} from all the collisions during the formation time. Deep in the LPM regime, there will be more and more scatterings in a formation time, and so $Q_{\perp} \gg q_{\perp}$.

In this same limit, the last term of (4.4) will dominate, and we can approximate

$$\delta E \simeq \frac{h^2}{2pkp'} \,. \tag{4.10}$$

We can also approximate the differences of F_s 's on the right-hand side of (4.3) by Taylor expansions, keeping the first term which does not integrate to zero by parity. The result is

$$2\mathbf{h} \simeq \frac{ih^{2}}{2pkp'}\mathbf{F}_{s}(\mathbf{h}; p', p, k) - \frac{g^{2}}{4} \left\{ \frac{1}{2}C_{A}p'^{2} + (C_{s} - \frac{1}{2}C_{A})k^{2} + \frac{1}{2}C_{A}p^{2} \right\} \times \nabla_{h}^{2}\mathbf{F}_{s}(\mathbf{h}; p', p, k) \int \frac{d^{2}q_{\perp}}{(2\pi)^{2}} q_{\perp}^{2} \mathcal{A}(q_{\perp}). \quad (4.11)$$

From (4.7), the remaining \mathbf{q}_{\perp} integral is logarithmically UV divergent. In the original integral, this divergence is cut off when our approximation that $\mathbf{h} + p'\mathbf{q}_{\perp}$ etc. are close to \mathbf{h} breaks down. Let $q_{\perp} \sim Q_{\perp 0}$ represent any rough estimate of this breakdown scale. Then, to leading order in logarithms,

$$\int \frac{d^2 q_{\perp}}{(2\pi)^2} q_{\perp}^2 \mathcal{A}(q_{\perp}) = T m_{\rm D}^2 \int \frac{d^2 q_{\perp}}{(2\pi)^2} \frac{1}{q_{\perp}^2 + m_{\rm D}^2} \simeq \frac{T m_{\rm D}^2}{4\pi} \ln(\hat{Q}_{\perp 0}^2), \tag{4.12}$$

where $\hat{Q}_{\perp 0} \equiv Q_{\perp 0}/m_{\rm D}$. The differential equation (4.11) for the leading-log approximation to $\mathbf{F}_s(\mathbf{h})$ can then be solved, applying the boundary conditions that \mathbf{F}_s remain finite at h=0 and $h\to\infty$. The result is¹⁰

$$\mathbf{F}_{s0}(\mathbf{h}) = i \, 4p'pk \left[\exp\left(-e^{\pm i\pi/4} \frac{h^2}{H_s^2}\right) - 1 \right] \frac{\mathbf{h}}{h^2}. \tag{4.13}$$

where

$$H_s^2 = \left\{ \frac{g^2}{2\pi} m_{\rm D}^2 T \left| p'pk \right| \left[\frac{1}{2} C_{\rm A} p'^2 + \left(C_s - \frac{1}{2} C_{\rm A} \right) k^2 + \frac{1}{2} C_{\rm A} p^2 \right] \ln(\hat{Q}_{\perp 0}^2) \right\}^{1/2}. \tag{4.14}$$

The \pm sign in (4.13) should be chosen as the sign of p'pk [which is negative in the case of (4.1b)], but this sign will not have any effect on our final answers. In terms of our previous qualitative discussion in Sec. II and qualitative identification of $h \sim PQ_{\perp}$, the above squared width H_s^2 of the distribution (4.13) is parametrically of order $H_s^2 \sim (PQ_{\perp})^2 \sim P^2 m_D^2 \hat{Q}_{\perp}^2$ with \hat{Q}_{\perp}^2 given by (2.12).

Plugging (4.13) into Eq. (4.2) for \mathcal{F}_s , one finds the leading-log approximation

$$\mathcal{F}_s \simeq \frac{d_s C_s \alpha}{(2\pi)^4} \sqrt{2} |p'pk| H_s^2. \tag{4.15}$$

In solving (4.11), it is convenient to use rotational invariance to first write \mathbf{F}_s as \mathbf{h} times a scalar function of h^2 .

Combining this with the equations (4.1) for the splitting functions γ gives the leading-log approximation to our result, which just corresponds to replacing all three logarithms on the right-hand side of (3.2) by $\ln(\hat{Q}_{\perp 0}^2)$:

$$\hat{\mu}_{\perp}^{2}(x_{1}, x_{2}, x_{3}; s_{1}, s_{2}, s_{3}) \simeq \frac{2H_{s}^{2}}{m_{D}^{2}P^{2}}$$

$$\simeq \frac{gT}{m_{D}} \left[\frac{2}{\pi} x_{1} x_{2} x_{3} \frac{P}{T} \right]^{1/2} \left\{ \left[\frac{1}{2} (C_{s_{2}} + C_{s_{3}} - C_{s_{1}}) x_{1}^{2} + \frac{1}{2} (C_{s_{3}} + C_{s_{1}} - C_{s_{2}}) x_{2}^{2} + \frac{1}{2} (C_{s_{2}} + C_{s_{3}} - C_{s_{1}}) x_{3}^{2} \right] \ln(\hat{Q}_{\perp 0}^{2}) \right\}^{1/2}. \tag{4.16}$$

Our leading-log result is the same as that derived by other authors,¹¹ which were based on general formalisms for the LPM effect but applied in a "static" approximation where the color fields of plasma particles were treated as simply screened by a Debye mass in the same way as static electric fields. In this approximation, the correlator $\mathcal{A}(q_{\perp})$ of (4.7) is replaced by¹²

$$\mathcal{A}_{\text{static}}(q_{\perp}) = \frac{Tm_{\text{D}}^2}{(q_{\perp}^2 + m_{\text{D}}^2)^2}.$$
(4.17)

The difference between this static approximation and the actual case is that the plasma screening of the non-static color electric and magnetic fields generated by moving plasma charges is different from the screening of the static, purely electric fields. However, the leading log result is generated by $q_{\perp} \gg m_{\rm D}$, and in this case all screening effects can be ignored. Accordingly, (4.17) is the same as (4.7) when $q_{\perp} \gg m_{\rm D}$. When we go to NLL order, individual momentum transfers q_{\perp} of order $m_{\rm D}$ will be important, and we will find a difference between a full treatment of plasma screening and the static approximation.

C. The NLL solution

To discuss the expansion, it is useful to introduce notation

$$(\mathbf{f}_1, \mathbf{f}_2) \equiv \int \frac{d^2h}{(2\pi)^2} \, \mathbf{f}_1(\mathbf{h}) \cdot \mathbf{f}_2(\mathbf{h})$$

$$(4.18)$$

for the inner product of two vector functions of \mathbf{h} . In this notation, the basic LPM equations (4.2) and (4.3) become

$$\mathcal{F} = \frac{d_s C_s \alpha}{2(2\pi)^3} \operatorname{Re}(\mathbf{S}, \mathbf{F}), \tag{4.19}$$

and

$$S = CF, (4.20)$$

In particular, our leading-log result for $d\Gamma_{g\to gg}/dx$ using (1.1), (3.1a) and (4.16) is the same as Eqs. (19–20) of Ref. [11] with their $\ln(\langle k_\perp^2 \rangle/m_D^2)$ identified as our $\ln(\hat{Q}_{\perp 0}^2)$.

^(19–20) of Ref. [11] with their $\ln(\langle k_{\perp}^2 \rangle/m_{\rm D}^2)$ identified as our $\ln(\hat{Q}_{\perp 0}^2)$. See, for example, Eq. (2.17) of Ref. [3]. The difference by an overall factor of πT is because they have normalized their version $V(q_{\perp}^2)$ of \mathcal{A} so that $\int d^2q_{\perp} \, V(q_{\perp}^2) = 1$. See also Ref. [15].

where we've defined the "source" S of the last equation by

$$S \equiv 2h \tag{4.21}$$

and C is a linear operator defined such that $C\mathbf{F}$ is the right-hand side of the LPM equation (4.3).

Let C_0 represent the approximation to C which gives the leading-log result. Expanding to first order in powers of $\delta C \equiv C - C_0$, we can write

$$(\mathbf{S}, \mathbf{F}) = (\mathbf{S}, C^{-1}\mathbf{S})$$

$$= (\mathbf{S}, C_0^{-1}\mathbf{S}) - (\mathbf{S}, C_0^{-1}\delta C C_0^{-1}\mathbf{S})$$

$$= 2(\mathbf{S}, C_0^{-1}\mathbf{S}) - (\mathbf{S}, C_0^{-1}C C_0^{-1}\mathbf{S})$$

$$= 2(\mathbf{S}, \mathbf{F}_0) - (\mathbf{F}_0, C\mathbf{F}_0),$$
(4.22)

and so

$$Re(\mathbf{S}, \mathbf{F}) = 2Re(\mathbf{S}, \mathbf{F}_0) - Re(\mathbf{F}_0, C\mathbf{F}_0). \tag{4.23}$$

The first term is just twice the leading-log result, which corresponds to

$$\operatorname{Re}(\mathbf{S}, \mathbf{F}_{0}) = \frac{\sqrt{2}}{\pi} |p'pk| H^{2}$$

$$= \frac{gm_{D}}{\pi} |p'pk|^{3/2} \left(\frac{T}{\pi}\right)^{1/2} \left\{ \left[\frac{1}{2}C_{A}p'^{2} + (C_{s} - \frac{1}{2}C_{A})k^{2} + \frac{1}{2}C_{A}p^{2}\right] \ln(\hat{Q}_{\perp 0}^{2}) \right\}^{1/2}.$$
(4.24)

We now need to compute

$$\operatorname{Re}(\mathbf{F}_0, C\mathbf{F}_0) = \operatorname{Re}I_1 + \frac{1}{2}C_A\operatorname{Re}I_2(p'^2) + (C_s - \frac{1}{2}C_A)\operatorname{Re}I_2(k^2) + \frac{1}{2}C_A\operatorname{Re}I_2(p^2),$$
 (4.25)

where

$$ReI_1 \equiv \int \frac{d^2h}{(2\pi)^2} Re[\mathbf{F}_0(\mathbf{h}) \cdot i \,\delta E(h) \,\mathbf{F}_0(\mathbf{h})]$$
(4.26)

and

$$I_2(\kappa^2) \equiv g^2 \int \frac{d^2h}{(2\pi)^2} \frac{d^2q_{\perp}}{(2\pi)^2} \mathcal{A}(q_{\perp}) \, \boldsymbol{F}_0(\boldsymbol{h}) \cdot \left[\boldsymbol{F}_0(\boldsymbol{h}) - \boldsymbol{F}_0(\boldsymbol{h} + \kappa \boldsymbol{q}_{\perp}) \right]. \tag{4.27}$$

In doing the I_1 integral, one can ignore the m^2 terms in Eq. (4.4) for δE and use the approximation (4.10). The m^2 terms in (4.4) are suppressed by order m^2P^2/h^2 compared to the h^2 term. In terms of the earlier qualitative discussion of section II, $h \sim PQ_{\perp}$, and so, from (2.13), this suppression factor is of order

$$\frac{m^2 P^2}{h^2} \sim \frac{m^2}{Q_\perp^2} \sim \frac{1}{\hat{Q}_\perp^2} \sim \left[\frac{P}{T} \ln \left(\frac{P}{T} \right) \right]^{-1/2}.$$
(4.28)

It is suppressed by a *power* of P/T, not simply a power of the logarithm $\ln(P/T)$, and so these mass terms do not contribute at any finite order in our inverse log expansion. The I_1 integral is trivial and then gives

Re
$$I_1 = \frac{3|p'pk|H^2}{\pi\sqrt{2}} = \frac{3}{2}\operatorname{Re}(\mathbf{S}, \mathbf{F}_0).$$
 (4.29)

The evaluation of I_2 is briefly outlined in the appendix and gives

$$I_2(\kappa^2) = -\frac{g^2 (p'pk)^2 T}{\pi^2} \int_0^\infty \frac{d\tau}{\tau} \left(1 - e^{-u_{\kappa}\tau}\right) \log\left(\frac{\tau + 1}{\tau}\right)$$
(4.30)

where

$$u_{\kappa} \equiv e^{\pm i\pi/4} \frac{m_{\rm D}^2 \kappa^2}{2H^2} \,. \tag{4.31}$$

Parametrically, u_{κ} is the same order as (4.28) and so is small compared to one. We therefore only need the small u_{κ} expansion of the integral (4.30),¹³ which is derived in the appendix:

$$I_2(\kappa^2) = -\frac{g^2(pkp')^2T}{\pi^2} (2 - \gamma_E - \ln u_\kappa) u_\kappa + O(u_\kappa^2), \tag{4.32}$$

and so

$$\operatorname{Re} I_2(\kappa^2) = -\frac{g^2(pkp')^2 T}{\pi^2 \sqrt{2}} \left(2 - \gamma_E + \frac{\pi}{4} - \ln|u_{\kappa}| \right) |u_{\kappa}| + O(u_{\kappa}^2). \tag{4.33}$$

Using (4.14) and (4.24), this can be rewritten as

$$\operatorname{Re} I_{2}(\kappa^{2}) = -\frac{1}{2} \operatorname{Re}(\mathbf{S}, \mathbf{F}_{0}) \frac{\kappa^{2} \ln \left(\frac{2\xi H_{s}^{2}}{m_{D}^{2}\kappa^{2}}\right)}{\left[\frac{1}{2}C_{A}p'^{2} + (C_{s} - \frac{1}{2}C_{A})k^{2} + \frac{1}{2}C_{A}p^{2}\right] \ln(\hat{Q}_{\perp 0}^{2})},$$
(4.34)

where ξ is the NLL constant under the log defined in (3.3). Putting our results for I_1 and I_2 into (4.23) and (4.25), the NLL result for Re(\mathbf{S}, \mathbf{F}) is

$$\operatorname{Re}(\boldsymbol{S}, \boldsymbol{F}_s) = \operatorname{Re}(\boldsymbol{S}, \boldsymbol{F}_0)$$

$$\times \frac{1}{2} \left\{ 1 + \frac{\frac{1}{2} C_{\mathcal{A}} p'^2 \ln\left(\frac{2\xi H_s^2}{m_{\mathcal{D}}^2 p'^2}\right) + (C_s - \frac{1}{2} C_{\mathcal{A}}) k^2 \ln\left(\frac{2\xi H_s^2}{m_{\mathcal{D}}^2 k^2}\right) + \frac{1}{2} C_{\mathcal{A}} p^2 \ln\left(\frac{2\xi H_s^2}{m_{\mathcal{D}}^2 p'^2}\right)}{\frac{1}{2} C_{\mathcal{A}} p'^2 \ln(\hat{Q}_{\perp 0}^2) + (C_s - \frac{1}{2} C_{\mathcal{A}}) k^2 \ln(\hat{Q}_{\perp 0}^2) + \frac{1}{2} C_{\mathcal{A}} p^2 \ln(\hat{Q}_{\perp 0}^2)} \right\}$$
(4.35)

with H_s given by (4.14). At leading-log order, where all logarithms are treated as the same, the multiplicative correction above simply reduces to a factor of one. At NLL order, its effect on the leading-log result (4.24) is simply to replace the curly brackets in (4.24) by the numerator of the big fraction in (4.35). This corresponds to the iterated NLL solution (3.7) quoted in section III, when the splitting functions γ are written in the form of (3.1). Note that H_s^2 in (4.35) depends on $\hat{Q}_{\perp 0}$. As mentioned earlier, the self-consistent equation (3.2) provides an answer which is equivalent at NLL order but which does not depend on specifying an initial guess $\hat{Q}_{\perp 0}$.

D. Dynamic vs. static treatment of screening

Since the static approximation (4.17) to screening is sometimes used in the literature, we will take a moment to discuss how the NLL order result would have been different had we

The exact result for (4.30) can be expressed (somewhat uselessly) in terms of the Meijer G function as $I_2(\kappa^2) = -\frac{g^2(p'pk)^2T}{\pi^2} \left[\frac{\pi^2}{4} + \frac{1}{2} \left(\gamma_{\rm E} + \ln u_\kappa \right)^2 - G_{2,3}^{3,1} \left(u_\kappa \left| \begin{smallmatrix} 0 & 1 & 1 \\ 0 & 0 & 1 \end{smallmatrix} \right. \right) \right].$

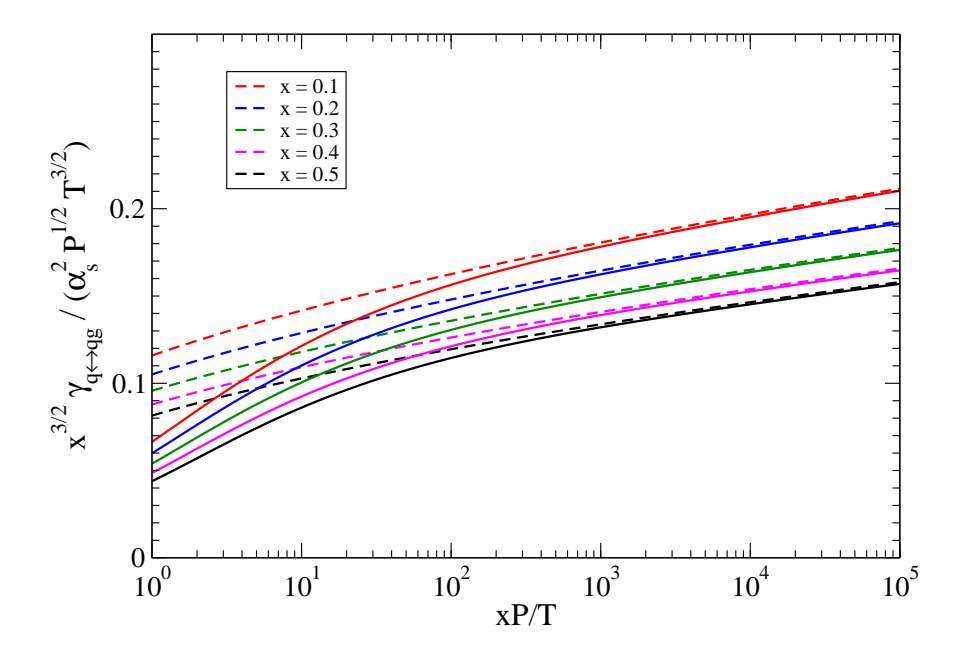


FIG. 4: Similar to Fig. 2 but for $\gamma_{q\leftrightarrow gq}$. x is the momentum fraction of the gluon.

made that approximation. This is simple to do by comparing with (4.7) and noting that

$$\mathcal{A}_{\text{static}} = m_{\text{D}}^2 \frac{\partial \mathcal{A}}{\partial (m_{\text{D}}^2)} = |u_{\kappa}| \frac{\partial \mathcal{A}}{\partial |u_{\kappa}|}, \qquad (4.36)$$

where the last equality uses (4.31) considering H as fixed. The only change comes in the calculation of I_2 . Applying (4.36) to (4.33),

$$\operatorname{Re} I_2(\kappa^2) \to \operatorname{Re} I_2^{\text{static}}(\kappa^2) = -\frac{g^2(pkp')^2T}{\pi^2\sqrt{2}} \left(1 - \gamma_{\text{E}} + \frac{\pi}{4} - \ln|u_{\kappa}|\right) |u_{\kappa}| + O(u_{\kappa}^2).$$
 (4.37)

This produces the same NLL result (3.2) as the fully dynamic case but with

$$\xi \to \xi_{\text{static}} \equiv \exp\left(1 - \gamma_{\text{E}} + \frac{\pi}{4}\right) \simeq 3.3474.$$
 (4.38)

V. NUMERICAL RESULTS

In the introduction, we have already discussed for $g \to gg$ the comparison of NLL results with a full computation at leading order in powers of α_s . The scaling in Fig. 2 was chosen by inspection of the small x limit of the NLL result given by (3.1) and (3.2), choosing powers of x so that the curves will be similar for small enough x. We give similar results for $\gamma_{q\to qg}$ and $\gamma_{g\to q\bar{q}}$ in Figs. 4 and 5. The fact that the small x curves in these figures do not fall closer together is because we have not quite gone to small enough x and because we have not bothered with factors of $\ln(1/x)$ in our consideration of how to scale the axis.

For the case of $q \to gq$, there is no final state symmetry that relates results for x to 1-x, so we show x > 0.5 results for this case in Fig. 6, scaled so that the curves are similar in the $1-x \to 0$ limit.

From these graphs, one can confirm for all splitting processes the general claim made in the introduction that the deviation of the NLL approximation from the full result at leading order in powers of α_s is roughly 20% or better for $p_{<} \gtrsim 10T$.

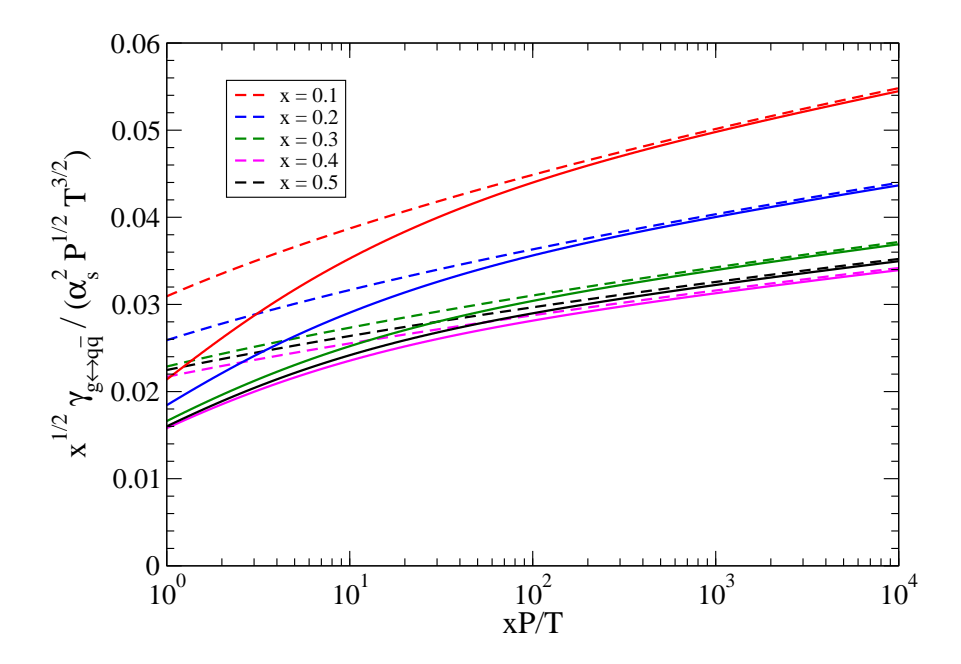


FIG. 5: Similar to Fig. 2 but for $\gamma_{g \leftrightarrow q\bar{q}}$.

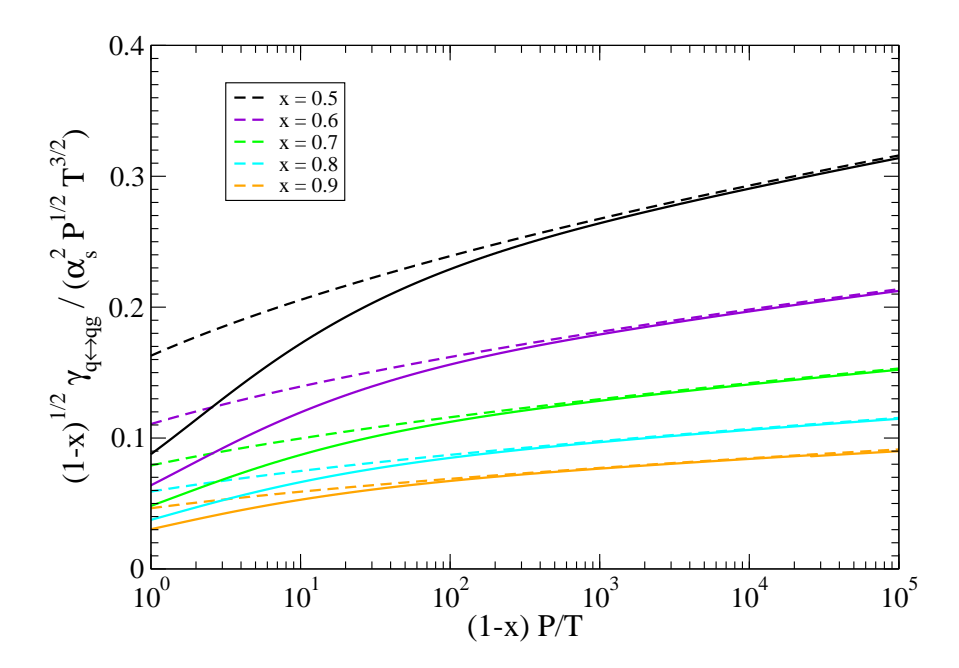


FIG. 6: The case $q \to gq$ for x > 0.5.

VI. THE CASE OF LARGE $\alpha_{\rm s} \ln(P/T)$

Throughout, we have assumed that α_s is small enough that we can ignore all effects suppressed by powers of α_s . In particular, we have ignored the issue of what renormalization scale α_s should be evaluated at: m_D , T, Q_\perp , or P? Formally,

$$\alpha_{\rm s}(\mu') = \alpha_{\rm s}(\mu) \left[1 + \beta_0 \alpha_{\rm s} \ln \left(\frac{\mu'^2}{\mu^2} \right) + O(\alpha_{\rm s}^2 \ln^2) \right], \tag{6.1}$$

and so we can ignore the ambiguity of scale choice if $\alpha_s \ln(\mu'/\mu)$ is small for relevant different possibilities μ and μ' .

In this paper, we have studied the deep LPM regime, where $\ln(Q_{\perp}/m_{\rm D}) \sim \ln(P/T)$ is large. Nonetheless, we have so far implicitly assumed that $\alpha_{\rm s} \ln(Q_{\perp}/m_{\rm D}) \sim \alpha_{\rm s} \ln(P/T)$ is small, since we have ignored all higher order corrections in $\alpha_{\rm s}$, including the running of the coupling constant. This assumption is also implicit in the full leading-order results of previous work, such as the LPM equation (4.3). However, in applications there could be a significant difference between $\alpha_{\rm s}(m_{\rm D})$ and $\alpha_{\rm s}(Q_{\perp})$ — that is, $\alpha_{\rm s} \ln(Q_{\perp}/m_{\rm D})$ may be large. In this section, we discuss what to do in that situation.

Earlier, we made the parametric assumption $P \ll T/[\alpha_{\rm s}^2 \ln(\alpha_{\rm s}^{-1})]$ in order to simplify the analysis of this paper, which is a first step towards computing the NLL result for the general case. With this assumption, the expansion parameter $\alpha_{\rm s} \ln(P/T)$ is never large in the weak coupling limit, since then $\alpha_{\rm s} \ln(P/T) \lesssim \alpha_{\rm s} \ln(\alpha_{\rm s}^{-2}) \ll 1$. In general, different choices of scale μ in $\alpha_{\rm s}(\mu)$ are formally not significant in the weak coupling limit if the different scales only differ by some power of the coupling. So, for example, there is no significant difference between $\alpha_{\rm s}(m_{\rm D})$ and $\alpha_{\rm s}(T)$ in the weak coupling limit.

In this section, we will abandon the restriction that $P \ll T/[\alpha_s^2 \ln(\alpha_s^{-1})]$ and consider extremely large P for which $\alpha_s(Q_\perp)$ may be significantly different than $\alpha_s(m_D) \simeq \alpha_s(T)$. We will correspondingly restrict ourself to a leading-log analysis, though now resumming the large factors of $\alpha_s \ln(Q_\perp/m_D)$ due to running of the coupling constant.

A. Large q_{\perp} behavior of $\mathcal{A}(q_{\perp})$

In our previous analysis, the leading-log result was dominated by $m_{\rm D} \ll q_{\perp}$, where the gauge field correlation function had the simple form

$$\mathcal{A}(q_{\perp}) \simeq \frac{T m_{\rm D}^2}{q_{\perp}^4} \qquad (m_{\rm D} \ll q_{\perp} \ll T).$$
 (6.2)

This can be understood as arising from the lower part of the scattering diagram of Fig. 3. The $1/q_{\perp}^4$ is the contribution $(-\omega^2 + q^2)^{-2}$ of the gauge propagator to the rate, with ω set equal to q^z as in the general definition (4.6) of $\mathcal{A}(q_{\perp})$. Setting $\omega = q^z$ is a reflection of energy conservation for the high-energy particle (the top solid line of Fig. 3) in the limit that $Q \ll P$. The factor of Tm_D^2 in (6.2) reproduces the contribution of the plasma particle and its phase space integral, integrated over q_z as in (4.6). It's appearance is more transparent if we write an explicit formula for the Debye mass,

$$Tm_{\rm D}^2 = g^2 \sum_s \nu_s t_{R_s} \int \frac{d^3 \ell}{(2\pi)^3} f_s(\ell) [1 \pm f_s(\ell)].$$
 (6.3)

Here one can see the g^2 associated with the contribution to the rate of the bottom vertex in Fig. 3, the Bose or Fermi distribution $f(\ell)$ for the probability of encountering a plasma particle with momentum ℓ , a final state Bose enhancement or Fermi blocking factor $1 \pm f(|\ell+q|) \simeq 1 \pm f(\ell)$, a sum over species s of the plasma particle, and the appropriate group factors and numbers of degrees of freedom.

For the opposite limit of $q_{\perp} \gg T$, one obtains a similar expression, but there is no final state factor $1 \pm f$. That's because if $\ell \sim T$ is a plasma particle momentum, and $q_{\perp} \gg T$,

then $|\ell + q| \gg T$ and so $1 \pm f(\ell + q) \simeq 1$. The form of $\mathcal{A}(q_{\perp})$ in this limit is

$$\mathcal{A}(q_{\perp}) \simeq \frac{g^2 \mathcal{N}}{q_{\perp}^4} \qquad (q_{\perp} \gg T),$$
 (6.4)

where

$$\mathcal{N} \equiv \sum_{s} \nu_s t_{R_s} \int \frac{d^3 \ell}{(2\pi)^3} f_s(\ell)$$
 (6.5)

is a measurement of the density of plasma particles, weighted by group factors. For QCD with $N_{\rm f}$ massless fermion flavors, $\mathcal N$ is

$$\mathcal{N} = \frac{\zeta(3)}{\zeta(2)} \left(t_{\rm A} + \frac{3}{2} N_{\rm f} t_{\rm F} \right) \frac{1}{3} T^3 = \frac{\zeta(3)}{\zeta(2)} \left(1 + \frac{1}{4} N_{\rm f} \right) T^3, \tag{6.6}$$

where $\zeta(s)$ is the Riemann zeta function. Compare this formula to (3.5) to see the difference between Tm_D^2 in (6.2) and $g^2\mathcal{N}$ in (6.4).

For 3-flavor QCD, $g^2\mathcal{N}$ is about 15% smaller than m_D^2T . For any phenomenologically relevant values of the coupling α_s , this difference is unlikely to be significant compared to other corrections, such as higher-order effects. So, one could reasonably just start from our earlier results based on the original formula (4.7) for $\mathcal{A}(T)$. However, the conceit of this paper is to work out precise results in the formal limit of arbitrarily weak coupling (and large logarithms), and so for sufficiently high energy jets we use (6.4).

Now consider our previous leading-log analysis. The Coulomb logarithm was generated from (4.12):

$$\int \frac{d^2 q_{\perp}}{(2\pi)^2} q_{\perp}^2 \mathcal{A}(q_{\perp}) \simeq \int_{\sim m_{\rm D}}^{\sim Q_{\perp}} \frac{q_{\perp} dq_{\perp}}{2\pi} \frac{T m_{\rm D}^2}{q_{\perp}^2} \simeq \frac{T m_{\rm D}^2}{2\pi} \ln\left(\frac{Q_{\perp}}{m_{\rm D}}\right) \qquad (Q_{\perp} \ll T). \tag{6.7}$$

For $Q_{\perp} \gg T$, there are instead two logarithmic contributions, coming from the different integration regions represented by (6.2) and (6.4):

$$\int \frac{d^2 q_{\perp}}{(2\pi)^2} q_{\perp}^2 \mathcal{A}(q_{\perp}) \simeq \frac{T m_{\rm D}^2}{2\pi} \ln\left(\frac{T}{m_{\rm D}}\right) + \frac{g^2 \mathcal{N}}{2\pi} \ln\left(\frac{Q_{\perp}}{T}\right) \qquad (Q_{\perp} \gg T)$$

$$\simeq \frac{(T m_{\rm D}^2 - g^2 \mathcal{N})}{2\pi} \ln\left(\frac{T}{m_{\rm D}}\right) + \frac{g^2 \mathcal{N}}{2\pi} \ln\left(\frac{Q_{\perp}}{m_{\rm D}}\right). \tag{6.8}$$

If $P \gg T/[\alpha_s^4 \ln(\alpha_s^{-1})]$, so that $Q_{\perp}/T \gg T/m_D$ by (2.9), then the second logarithm dominates. Since in this section we will be interested in P large enough that there is significant running of the coupling constant (and so formally P larger than T times any fixed power of $1/\alpha_s$), we shall henceforth assume this is the case. If we ignored the running of the coupling, we'd have

$$\int \frac{d^2 q_{\perp}}{(2\pi)^2} q_{\perp}^2 \mathcal{A}(q_{\perp}) \simeq \int_{\sim m_{\rm D}}^{\sim Q_{\perp}} \frac{q_{\perp} dq_{\perp}}{2\pi} \frac{g^2 \mathcal{N}}{q_{\perp}^2} \simeq \frac{g^2 \mathcal{N}}{2\pi} \ln\left(\frac{Q_{\perp}}{m_{\rm D}}\right) \qquad \left(Q_{\perp} \gg \frac{T}{\alpha_{\rm s}^4 \ln(\alpha_{\rm s}^{-1})}\right) \quad (6.9)$$

in this case. Given our assumpations and approximations, we could have just as well made the lower limit T instead of $m_{\rm D}$ in (6.9). However, because of the small difference between $g^2\mathcal{N}$ and $m_{\rm D}^2T$, taking the lower limit to be $m_{\rm D}$ is probably slightly better in practice.

B. Running of coupling with q_{\perp}

We begin with a discussion of the scale of the coupling g in the $g^2\mathcal{A}(q_\perp;g^2)$ factor in the LPM equation (4.3), where we now write $\mathcal{A}(q_\perp;g^2)$ instead of $\mathcal{A}(q_\perp)$ to emphasize the fact that \mathcal{A} depends on g^2 , e.g. as in (6.4). Physically, this factor is proportional to the rate for a high-energy particle to scatter off of a plasma particle, with momentum transfer q_\perp . (See, for example, the discussion in Ref. [8].) A momentum transfer of q_\perp corresponds to an impact parameter between the high-energy particle and the plasma particle of order $1/q_\perp$. If this distance is very, very small, then g^2 in this Coulomb scattering amplitude should be correspondingly smaller because of the anti-screening of the QCD vacuum. (For $1/q_\perp \ll$ the Debye screening length $1/m_D$, medium effects are ignorable, and so the relevant consideration for such a collision is of the running coupling constant in vacuum.) The upshot is that the appropriate scale for g^2 in this scattering rate should be set by q_\perp . This is precisely what we would get by summing up all 1-loop bubbles on the exchanged gluon line. We therefore expect that the LPM equation (4.3) should be modified by replacing g^2 by $g^2(q_\perp)$ so that it becomes

$$2\boldsymbol{h} = i \,\delta E(\boldsymbol{h}; p', p, k) \,\boldsymbol{F}_s(\boldsymbol{h}; p', p, k) + \int \frac{d^2 q_\perp}{(2\pi)^2} \,g^2(q_\perp) \,\mathcal{A}(q_\perp; g^2(q_\perp)) \Big\{\cdots\Big\}. \tag{6.10}$$

This is the same prescription as used in a related context by Peshier in an analysis of collisional energy loss [16].

Now repeat the leading-log analysis we reviewed in Section IV B. Correspondingly, we'll use the 1-loop renormalization group result for $g^2(q_{\perp})$,

$$g^{2}(\mu) = \frac{1}{-\bar{\beta}_{0} \ln(\mu^{2}/\Lambda^{2})}.$$
(6.11)

For QCD, Λ represents $\Lambda_{\rm QCD}$, and

$$\bar{\beta}_0 = -\frac{(11C_A - 4N_f t_F)}{48\pi^2} = -\frac{(33 - 2N_f)}{48\pi^2} < 0. \tag{6.12}$$

(For QED, Λ represents the ultraviolet Landau pole, and $\bar{\beta}_0 > 0$.) The integral analogous to g^2 times (6.9) is

$$\int \frac{d^{2}q_{\perp}}{(2\pi)^{2}} g^{2}(q_{\perp}) q_{\perp}^{2} \mathcal{A}(q_{\perp}; g^{2}(q_{\perp})) \simeq \int_{\sim m_{D}}^{\sim Q_{\perp}} \frac{q_{\perp} dq_{\perp}}{2\pi} \frac{g^{4}(q_{\perp})\mathcal{N}}{q_{\perp}^{2}}
\simeq \frac{\mathcal{N}}{8\pi \bar{\beta}_{0}^{2}} \int_{\sim m_{D}}^{\sim Q_{\perp}} \frac{dq_{\perp}}{q_{\perp} \ln^{2}(q_{\perp}/\Lambda)}
= \frac{\mathcal{N}}{8\pi \bar{\beta}_{0}^{2}} \left[\frac{1}{\ln(m_{D}/\Lambda)} - \frac{1}{\ln(Q_{\perp}/\Lambda)} \right].$$
(6.13)

Following through the previous leading-log derivation, we will get the same result for F_0 and H but with the replacement

$$g^2 m_{\rm D}^2 T \ln(\hat{Q}_{\perp 0}^2) \to \frac{\mathcal{N}}{2\bar{\beta}_0^2} \left[\frac{1}{\ln(m_{\rm D}/\Lambda)} - \frac{1}{\ln(Q_{\perp 0}/\Lambda)} \right] = \mathcal{N} \frac{[g^2(m_{\rm D}) - g^2(Q_{\perp 0})]}{-\bar{\beta}_0}$$
 (6.14)

in (4.14). The correspondence with the original leading-log result is easier to see if we use (6.11) to rewrite this in the equivalent form

$$g^2 m_{\rm D}^2 T \ln(\hat{Q}_{\perp 0}^2) \to g^2(m_{\rm D}) g^2(Q_{\perp}) \mathcal{N} \ln(\hat{Q}_{\perp 0}^2).$$
 (6.15)

It is interesting to note that, because of asymptotic freedom in QCD, the running-coupling formula on the right-hand side of (6.14) is finite as P (and so Q_{\perp}) becomes infinite. In this limit, the value of $\alpha_{\rm s}(Q_{\perp})$ is irrelevant—a fact slightly obscured by (6.15) but made clear by (6.14). In this case, the momentum transfers q_{\perp} in individual $2\rightarrow 2$ scatterings which dominate the integral (6.13) range, roughly speaking, from T up to those where $\alpha_{\rm s}(q_{\perp})$ can first be considered small compared to $\alpha_{\rm s}(T)$. In particular, once Q_{\perp} is large enough, the scale of q_{\perp} does not continue to grow as one increases P and Q_{\perp} .

C. Remaining g^2 and synthesis

There remains one other factor of g^2 in the problem, which is the cost for emitting the energetic, bremsstrahlung particle. Because of the LPM effect, a bremsstrahlung gluon cannot resolve individual $2\rightarrow 2$ collisions with the plasma but is only sensitive to the net deflection of the high energy particles over the entire formation time. The relevant scale for the g^2 cost of bremsstrahlung is therefore plausibly the total momentum transfer¹⁴ (2.13) $Q_{\perp} \sim m_{\rm D}(P/T)^{1/4} \ln^{1/4}(P/T)$. [We will ignore the issue of whether this last P should be P or xP or (1-x)P but will assume that x and 1-x are large enough that there is not much difference in $\alpha_{\rm s}$.] We therefore propose that the correct leading-log formula in the case of small $\alpha_{\rm s}$ but large $\alpha_{\rm s} \ln(P/T)$ is given by (i) replacing $\alpha_{\rm s}$ by $\alpha_{\rm s}(Q_{\perp}) \simeq \alpha_{\rm s}(m_{\rm D}\hat{Q}_{\perp 0})$ in (3.1), and then (ii) using (6.14) to replace (4.16) by

$$\mu_{\perp}^{2} \equiv m_{\mathrm{D}}^{2} \hat{\mu}_{\perp}^{2} \simeq (T\mathcal{N})^{1/2} \left[\frac{2}{\pi} x_{1} x_{2} x_{3} \frac{P}{T} \right]^{1/2}$$

$$\times \left[\frac{1}{2} (C_{s_{2}} + C_{s_{3}} - C_{s_{1}}) x_{1}^{2} + \frac{1}{2} (C_{s_{3}} + C_{s_{1}} - C_{s_{2}}) x_{2}^{2} + \frac{1}{2} (C_{s_{2}} + C_{s_{3}} - C_{s_{1}}) x_{3}^{2} \right]^{1/2}$$

$$\times \left[\frac{g^{2} (m_{\mathrm{D}}) - g^{2} (Q_{\perp 0})}{-\bar{\beta}_{0}} \right]^{1/2}$$

$$(6.16)$$

[Note that it is the combination $\mu_{\perp}^2 = m_{\rm D}^2 \hat{\mu}_{\perp}^2$ which appears in (3.1).] Here, $Q_{\perp 0}$ is chosen with order of magnitude given by (2.13), or one could simply self-consistently choose $Q_{\perp 0} = \mu_{\perp}$.

For the case of large $g^2 \ln(\hat{Q}_{\perp 0}^2)$, there is not an obvious benefit to pushing further to find the NLL solution to the running LPM equation (6.10). For large $g^2 \ln(\hat{Q}_{\perp 0}^2)$, the expansion

 $^{^{14}}$ $1/Q_{\perp}$ is the transverse distance corresponding to the deflection of the high-energy particle due to $2\rightarrow 2$ scatterings during a formation time. To see this, consider that if the particle picks up transverse momentum Q_{\perp} in that time, then it's transverse velocity will be of order Q_{\perp}/P . Multiplying this transverse velocity by a formation time $t_{\text{form}} \sim P/Q_{\perp}^2$ (2.4) then gives $1/Q_{\perp}$. The same scale is also the scale of the quantum mechanical uncertainty of the transverse position during a formation time (which is why LPM interference can occur). In contrast, the scale $1/q_{\perp}$ relevant to section VIB is the typical transverse distance between the high energy particle and the plasma particles it is scattering from.

parameter $[\ln(Q_{\perp}/m_{\rm D})]^{-1}$ is parametrically the same order as $\alpha_{\rm s}$, and so one cannot obviously justify neglecting corrections that are higher order in $\alpha_{\rm s}$ that have not been included in the running of the coupling. On the other hand, it would be nice to have a single, well-defined formula that interpolated our previous NLL result into the realm of large $g^2 \ln(\hat{Q}_{\perp 0}^2)$. But we shall not pursue this here.

We have made plausibility arguments about which renormalization scales should be used for evaluating the coupling g^2 . It's possible, however, that if one starts looking at corrections suppressed by α_s that there are other large logarithms which arise, unrelated to the runnings we have described. To settle the issue definitely, it would be nice to have explicit weak-coupling calculations beyond leading order in α_s of a well-defined physical quantity that is dominated by particle splitting processes.

Acknowledgments

We are indebted to Guy Moore who, after reading the original version of this manuscript, pointed out to us that our analysis of the NLL result breaks down for $p \gtrsim T/[\alpha_{\rm s}^2 \ln(\alpha_{\rm s}^{-1})]$, and that the same effect required corrections to our analysis of Sec. VI. We are also indebted to the referee, who led us to realize another error in our original analysis of Sec. VI concerning our treatment of the running coupling. We also thank Yuri Kovchegov for useful and interesting conversations, and in particular for pointing out to us that the Coulomb logarithm for the case of running coupling constants can be written in the form of (6.15). This work was supported, in part, by the U.S. Department of Energy under Grant No. DE-FG02-97ER41027.

APPENDIX A: I2

1. The I_2 integral

Here is one way to do the integral $I_2(\kappa^2)$ of (4.27). First use the standard trick of rewriting

$$\frac{1}{q^2 + m^2} = \int_0^\infty d\lambda \, e^{-\lambda(q^2 + m^2)},\tag{A1}$$

so that

$$I_{2}(\kappa^{2}) = g^{2}T \int_{0}^{\infty} d\lambda \int \frac{d^{2}h}{(2\pi)^{2}} \frac{d^{2}q_{\perp}}{(2\pi)^{2}} \left[e^{-\lambda q_{\perp}^{2}} - e^{-\lambda(q_{\perp}^{2} + m_{D}^{2})} \right] \boldsymbol{F}_{0}(\boldsymbol{h}) \cdot \left[\boldsymbol{F}_{0}(\boldsymbol{h}) - \boldsymbol{F}_{0}(\boldsymbol{h} + \kappa \boldsymbol{q}_{\perp}) \right]. \tag{A2}$$

Next rewrite (4.13) in the form

$$\mathbf{F}_0(\mathbf{h}) = C\left(e^{-Ah^2} - e^{-\epsilon h^2}\right) \frac{\mathbf{h}}{h^2},\tag{A3}$$

where C = i4p'pk, $A = e^{\pm i\pi/4}/H^2$, and the limit $\epsilon \to 0^+$ is taken at the end of the day. By introducing ϵ , we can split I_2 into

$$I_2(\kappa^2) = \mathcal{I}(0) - \mathcal{I}(\kappa^2), \tag{A4}$$

where

$$\mathcal{I}(\kappa^2) = g^2 T \int_0^\infty d\lambda \left(1 - e^{-\lambda m_D^2} \right) \int \frac{d^2 h}{(2\pi)^2} \frac{d^2 j}{(2\pi)^2 \kappa^2} e^{-\lambda j^2/\kappa^2} \boldsymbol{F}_0(\boldsymbol{h}) \cdot \boldsymbol{F}_0(\boldsymbol{h} + \boldsymbol{j})$$
(A5)

and we have introduced the notation $j \equiv -\kappa q_{\perp}$. The integral \mathcal{I} would be divergent if we had not introduced some sort of regulator like the ϵ . Now note that (A5) has the form of a convolution, and so by Fourier transformation we can recast it as a single two-dimensional integral over a Fourier conjugate variable which we'll call \boldsymbol{B} . Two-dimensional Fourier transformation of \boldsymbol{h} or \boldsymbol{j} takes

$$F_0(h) \to -\frac{iCB}{2\pi B^2} \left(e^{-B^2/4A} - e^{-B^2/4\epsilon} \right),$$
 (A6)

$$e^{-\lambda j^2/\kappa^2} \to \frac{\kappa^2}{4\pi\lambda} e^{-\kappa^2 B^2/4\lambda},$$
 (A7)

and so the integral becomes

$$\mathcal{I}(\kappa^2) = \frac{g^2 C^2 T}{16\pi^3} \int_0^\infty \frac{d\lambda}{\lambda} (1 - e^{-\lambda m_{\rm D}^2}) \int \frac{d^2 B}{B^2} e^{-\kappa^2 B^2/4\lambda} \left(e^{-B^2/4A} - e^{-B^2/4\epsilon} \right)^2. \tag{A8}$$

By (A4), then

$$I_2(\kappa^2) = \frac{g^2 C^2 T}{16\pi^3} \int_0^\infty \frac{d\lambda}{\lambda} (1 - e^{-\lambda m_D^2}) \int \frac{d^2 B}{B^2} (1 - e^{-\kappa^2 B^2/4\lambda}) \left(e^{-B^2/4A} - e^{-B^2/4\epsilon} \right)^2.$$
 (A9)

We can now safely take the limit $\epsilon \to 0$, giving

$$I_2(\kappa^2) = \frac{g^2 C^2 T}{16\pi^3} \int_0^\infty \frac{d\lambda}{\lambda} (1 - e^{-\lambda m_D^2}) \int \frac{d^2 B}{B^2} (1 - e^{-\kappa^2 B^2/4\lambda}) e^{-B^2/2A}.$$
 (A10)

Finally, doing the **B** integral and changing variables from λ to $\tau \equiv 2\lambda/A\kappa^2$ gives (4.30).

2. Small u_{κ} expansion

To expand (4.30) in powers of u_{κ} , it is convenient to notice that $I_2(0) = 0$ and then instead expand

$$\frac{\partial I_2}{\partial u_{\kappa}} = -\frac{g^2 (p'pk)^2 T}{\pi^2} \int_0^{\infty} d\tau \, e^{-u_{\kappa}\tau} \log\left(\frac{\tau + 1}{\tau}\right)
= -\frac{g^2 (p'pk)^2 T}{\pi^2} \frac{\left[\gamma_{\rm E} + \ln u_{\kappa} - e^{u_{\kappa}} \operatorname{Ei}(-u_{\kappa})\right]}{u_{\kappa}},$$
(A11)

where Ei is the exponential integral. The small u_{κ} expansion is

$$\frac{\partial I_2}{\partial u_{\kappa}} = -\frac{g^2 (p'pk)^2 T}{\pi^2} \left(1 - \gamma_{\rm E} - \ln u_{\kappa}\right). \tag{A12}$$

Integrating both sides and using $I_2(0) = 0$ then yields (4.32).

^[1] B. G. Zakharov, JETP Lett. **65**, 615 (1997) [hep-ph/9704255]; **63**, 952 (1996) [hep-ph/9607440];

- [2] R. Baier, Y. L. Dokshitzer, A. H. Mueller, S. Peigne and D. Schiff, Nucl. Phys. B 478, 577 (1996) [arXiv:hep-ph/9604327];
- [3] R. Baier, Y. L. Dokshitzer, A. H. Mueller, S. Peigne and D. Schiff, Nucl. Phys. B **483**, 291 (1997) [arXiv:hep-ph/9607355];
- [4] R. Baier, Y. L. Dokshitzer, A. H. Mueller and D. Schiff, Nucl. Phys. B 531, 403 (1998)
 [arXiv:hep-ph/9804212]; R. Baier, Y. L. Dokshitzer, A. H. Mueller, S. Peigne and D. Schiff,
 484, 265 (1997) [arXiv:hep-ph/9608322].
- [5] R. Baier, D. Schiff and B. G. Zakharov, Ann. Rev. Nucl. Part. Sci. **50**, 37 (2000) [arXiv:hep-ph/0002198];
- [6] S. Jeon and G. D. Moore, Phys. Rev. C 71, 034901 (2005) [arXiv:hep-ph/0309332].
- [7] A. B. Migdal, Phys. Rev. **103**, 1811 (1956);
- [8] P. Arnold, G. D. Moore and L. G. Yaffe, JHEP **0206**, 030 (2002) [arXiv:hep-ph/0204343].
- [9] P. Arnold, G. D. Moore and L. G. Yaffe, JHEP **0301**, 030 (2003) [arXiv:hep-ph/0209353].
- [10] P. Arnold, G. D. Moore and L. G. Yaffe, JHEP **0305**, 051 (2003) [arXiv:hep-ph/0302165].
- [11] R. Baier, A. H. Mueller, D. Schiff and D. T. Son, Phys. Lett. B **502**, 51 (2001) [arXiv:hep-ph/0009237].
- [12] P. Arnold, Int. J. Mod. Phys. E 16, 2555 (2007) [arXiv:0708.0812 [hep-ph]].
- [13] E. M. Lifshitz and L. P. Pitaevskii, *Physical Kinetics* (Pergamon, 1981).
- [14] P. Aurenche, F. Gelis and H. Zaraket, JHEP **0205**, 043 (2002) [arXiv:hep-ph/0204146].
- [15] M. Djordjevic and U. Heinz, Phys. Rev. C 77, 024905 (2008) [arXiv:0705.3439 [nucl-th]].
- [16] A. Peshier, J. Phys. G **35**, 044028 (2008).